Flow phenomena in soils with small permeability

Phénomènes d'écoulement dans des sols peu perméables

H. NENDZA, O. Prof. Dr.-Ing., Foundation Engineering and Soil Mechanics Section, University of Essen, FRG
H.-G. GABENER, Dr.-Ing., Foundation Engineering and Soil Mechanics Section, University of Essen, FRG

SYNOPSIS Deviations from Darcy's Law have been observed for the flow of water in moderately permeable, cohesive soils. The permeability coefficients, so-called initial gradients i_0, and boundaries between the linear and pre-linear zones of flow determined as a function of pore ratio and clay content are stated. Discussed are the effects of the laws of filtration observed in connection with flow phenomena in foundation soils, especially in regard to flow nets and hydraulic failure.

INTRODUCTION

Generally, Darcy's Law is also a basis for the calculation of flow phenomena occurring in fine-grained, cohesive soils. However, it is now a well known fact that a flow behaviour deviating from Darcy's Law is encountered in the case of moderately permeable soil material.

DEVIATIONS FROM DARCY's LAW IN THE CASE OF COHESIVE SOILS

For flow phenomena occurring in cohesive soils, the law of filtration

$$v = k \cdot (i - i_0) \qquad (1)$$

is taken as a basis, provided that linearity exists between the hydraulic gradient i and the discharge velocity v, whereas in the so-called pre-linear zone, functions of the power series are used (Hansbo, 1960).

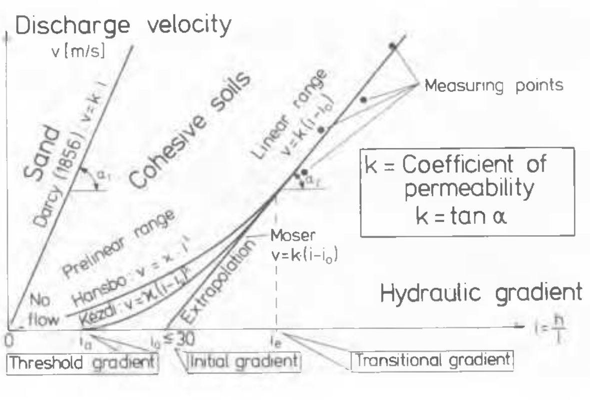

Fig. 1 Deviations from Darcy's Law in the case of cohesive soils according to Hansbo, Kézdi, and Moser

Deviations in the linear zone of flow

In contrast to Darcy's Law, the straight line of the linear zone of flow no longer intersects the reference point of the co-ordinate system but constitutes an intersection with the axis of the gradient. The appurtenant section of the axis is being defined as i_0 and is called inital gradient. i_0 is determined by extending

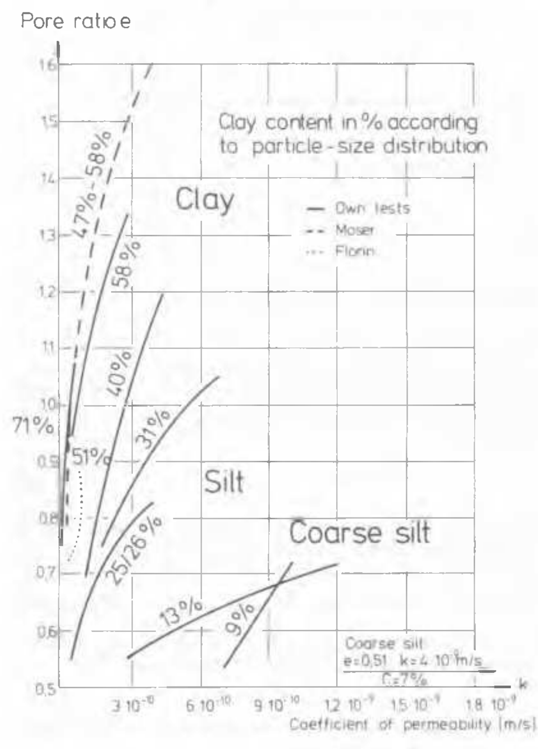

Fig. 2 Interrelation between the permeability coefficients of cohesive soils studied and their pore ratios and clay contents

the section of the straight line defined by measuring points in the direction of the i-axis, i.e. by extrapolation.

Extensive permeability studies carried out by the University of Essen have shown that the permeability coefficient k, according to equation (1), is a function of the clay content of the soil material and of its pore ratio (see Fig. 2).

The initial gradients i_0, on their account, are a function of the pertaining permeability coefficients k of cohesive soils and, consequently, are also a function of the clay content and pore ratio (see Fig. 3).

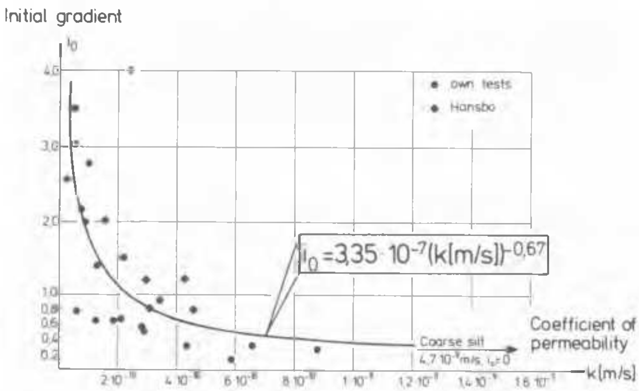

Fig. 3 Interrelation between the permeability coefficients k and initial gradients i_0 of cohesive soils studied

The initial gradients were determined as a function of the type of soil, as follows:

Coarse-grained silt	$0 \leqq i_0 \leqq 0.5$
Silt	$0.3 \leqq i_0 \leqq 1.7$
Clay	$0.4 \leqq i_0 \leqq 3.7$

Deviations in the pre-linear zone of flow

At levels below gradient i_e, as in Fig. 1, permeability gradually decreases with declining hydraulic gradient. To describe this phenomenon, it is commonly suggested to use the power series function

$$v = \varkappa \cdot i^{\lambda} \qquad (2)$$

According to Hansbo (1960), the parabola resulting therefrom, when plotted on a graph, lies tangentially to the straight line $v = k\,(i - i_0)$ at the point of intersection i_e. At the origin of the co-ordinate system according to Fig. 1, the i-axis represents the tangent to the parabola.

Own tests have resulted, however, in the curve pattern portrayed in Fig. 4. In accordance therewith, the slope of the round-off parabola at the origin of the co-ordinates becomes zero only in the case of clay material with very moderate permeability properties. For clay material

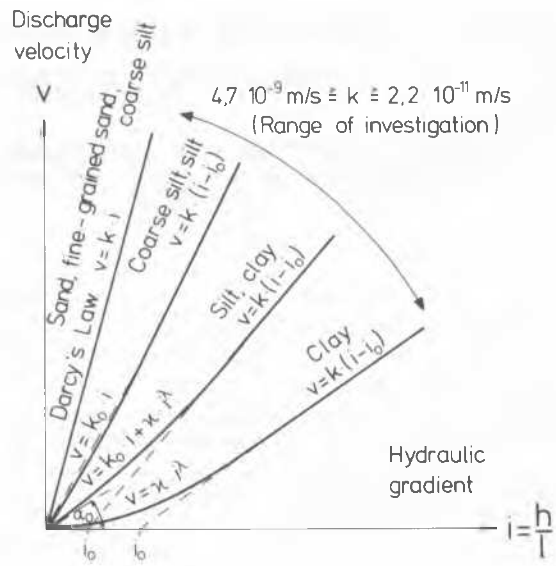

Fig. 4 Correlation between types of soil and relevant filtration laws

with better permeability properties and for silt, the angle α_0 results between the tangent to the parabola at the zero point and the axis of the gradient. It is therefore suggested that such a curve pattern be described by an equation written as follows:

$$v = k_0 \cdot i + \varkappa \cdot i^{\lambda} \qquad (3)$$

In the case of coarse-grained silt, the curve pattern in the pre-linear zone hardly showed any flexure. On the other hand, the angle α_0 entered the picture to an even greater extent. For this, the linear relation

$$v = k_0 \cdot i \qquad (4)$$

can be used.

The flow tests were carried out at high water saturation levels of the samples and covered the range $4.7 \cdot 10^{-9}$ m/s $\geqq k \geqq 2.2 \cdot 10^{-11}$ m/s. In these tests, flowless zones could in no case be observed.

BOUNDARY BETWEEN THE LINEAR AND PRE-LINEAR ZONES OF FLOW IN COMPARISON WITH GRADIENTS VALID FOR FLOWS IN REAL NATURE

Transition from the linear to the pre-linear zone of flow takes places at a point called transitional gradient i_e. Fig. 5 shows the values which have been determined for the cohesive soil material tested as a function of their clay content und pore ratio.

In the case of flow phenomena present in homogeneous foundation soil, e. g. in the presence of water circulating around an impervious building pit wall, the hydraulic gradients take a value less than 1. Only in the case of

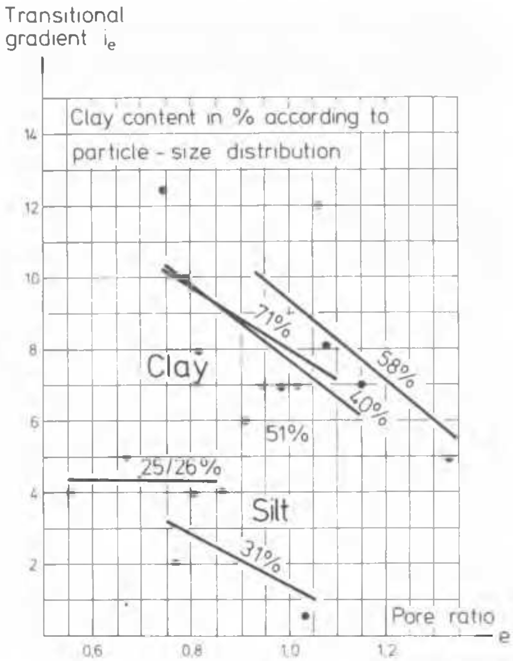

Fig. 5 Boundary between the linear and pre-linear zones of flow as a function of clay content and pore ratio

a great amount of free surface water, gradients above 1 are possible. A comparison with Fig. 5 clearly shows that water movement of this type occurs in most cases in the pre-linear zone of flow for which the equations (2), (3), or (4) have been written. Flow phenomena in the linear zone which would be permissive of stating equation (1) are more likely to be expected for a stratified foundation soil configuration in the less permeable layers.

HYDRAULIC FAILURE IN COHESIVE SOILS

An upward movement of water towards ground level or building pit bottom may result in hydraulic failure. The safety checking procedures for hydraulic failure are in most cases designed for non-cohesive soils, but they are also used for cohesive foundation soils. Practical experience and theoretical considerations also have shown that there is a lesser risk of hydraulic failure in the latter case. Reduced permeability in the pre-linear zone of flow or the absence of water movement below the threshold or initial gradient, respectively, cannot be the reason for this.

Assuming the existence of a flowless zone below gradient i_0 or gradient i_a as per Fig. 1, under a stationary state condition with $i < i_a < i_0$ the seepage pressure is replaced by a "spatial supporting pressure" as is experienced in the case of slurry trenches (Müller-Kirchenbauer, 1972). This description is meant to say that the transmission of the pore water pressure to the surrounding soil particles takes place at a slow pace and not to its full extent at an assumed impervious membrane wall. The specific supporting pressure analogous to the specific seepage pressure is as shown below:

$$\text{for } i = i_0 : j = \gamma_w \cdot i_0 \quad (5)$$

$$\text{for } i = i_a : j = \gamma_w \cdot i_a \quad (6)$$

$$\text{for } i \gtrless i_a \gtrless i_0 : j = \gamma_w \cdot i \quad (7)$$

In addition to this, it can be assumed on the basis of the permeability tests performed that the water moves in cohesive soils even in the presence of low hydraulic gradients and that seepage pressure in its common form thus ensues in the majority of cases.

The reason of the better stability of cohesive soils against hydraulic failure becomes evident when the proof furnished by Terzaghi/Peck (1961) is extended by the statement of forces forwarded by Davidenkoff (1970). For this, in addition to the weight W of the body of earth under uplift both the cohesion of the lateral faces and the tensile strength of the bottom face are also stated:

$$F = \frac{W + C_1 + C_2 + T}{J} \quad (8)$$

$$F = \frac{d \cdot b \cdot \gamma' + (c_1 + c_2) \cdot d + c_0 \cdot b}{d \cdot b \cdot \gamma_w \cdot i_{av.}} \quad (9)$$

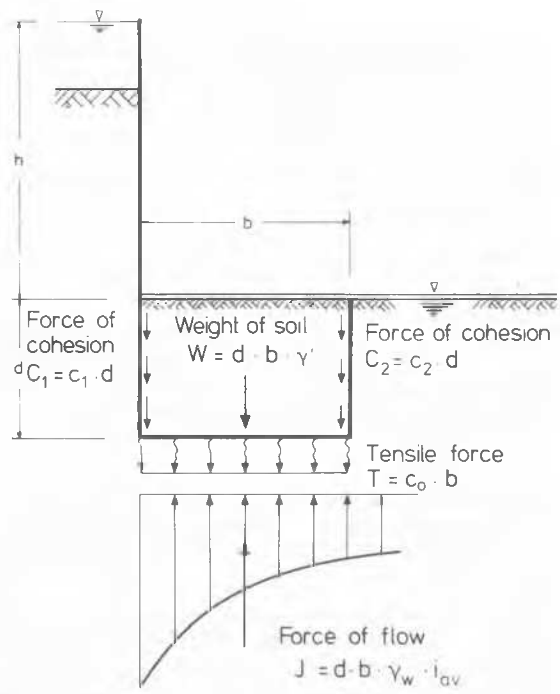

Fig. 6 Possible statement of forces for homogeneous cohesive soils

The forces stated are dependent on the width b of the body of earth under uplift or on its depth d, respectively, or on both dimensions. To determine the applicable type of body under uplift for the example shown in Fig. 7, several soil bodies ahead of the base of the wall were checked and the safety was plotted against the hydraulic failure shown in Fig. 8 as a function of the width-/depth ratio b/d.

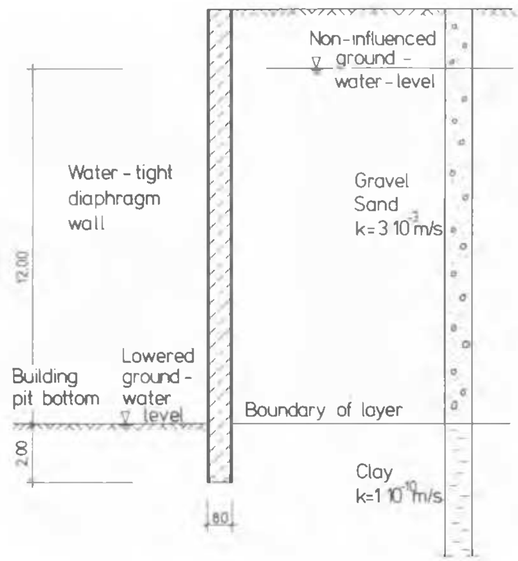

Fig. 7 Example for proof of safety against hydraulic failure

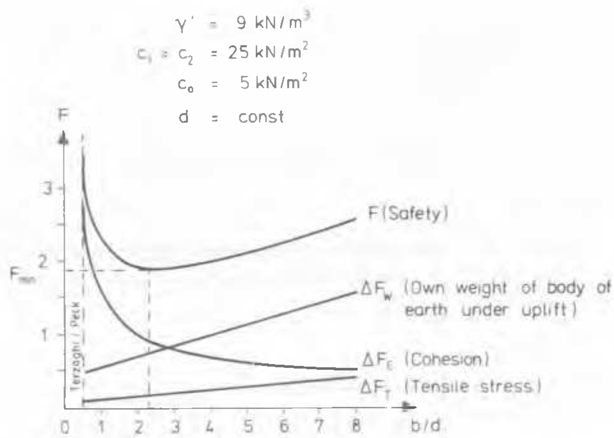

Fig. 8 Change of safety against hydraulic failure as a function of the lateral aspect ratio of the body of earth under uplift

From Fig. 8 it appears that the lowest amount of safety F_{min} for a body under uplift is attained with $b \approx 2.3 \cdot d$ and that proof being furnished for the body under uplift with $b = 0.5 \cdot d$ according to Terzaghi/Peck in connection with equations (8) and (9) will lead to faulty findings. The safety F according to Fig. 8 is brought about by the own weight of the body of soil, through cohesion and through tensile strength:

$$F = \Delta F_W + \Delta F_C + \Delta F_T \qquad (10)$$

The safety F_{min} is essentially composed of the effects of own weight and cohesion. The effect of tensile strength, inclusion of which appears to be problematic anyhow, is insignificant and should not be taken into account.

The traditional testing procedures developed for non-cohesive soils, when applied to cohesive soils, give safeties of $0.43 \leqq F \leqq 0.60$, thus, far below 1 for the cross-section shown in Fig. 7. However, since the sheeting in Fig. 7 represents a structure actually carried out and shows no failure, the stability, on account of cohesion, must have been $\geqq 1$.

FLOW NETS IN THE CASE OF CHANGED LAWS OF FILTRATION

The average flow gradient in equation (9) can be determined with the aid of a flow net. The flow and potential lines represent the solutions of the Laplace differential equation and these, on their turn, include Darcy's relationships. Using the equation (1) the Laplace differential equation is derived also, because the constant i_0 becomes zero when differentiating. However, this must not lead to the conclusion that the same flow net is obtained using both filtration laws, because the boundary conditions are subject to changes. As an example, Fig. 9 shows an impervious boundary. From the condition that the discharge velocity perpendicular to the boundary equals zero it follows according to Darcy's Law that the corresponding hydraulic gradient also becomes zero. However, according to equation (1) it results that the hydraulic gradient can assume the magnitude of the initial gradient.

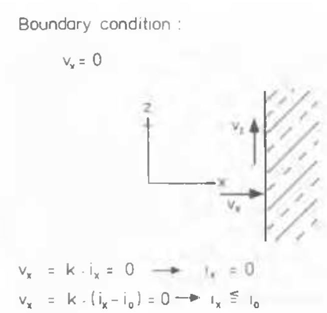

Fig. 9 Boundary conditions at the impervious contour line of a structure

The statement of the power series function (2) in the pre-linear zone of flow gives the differential equation

$$\varkappa \cdot \lambda \left(\frac{\partial h}{\partial x}\right)^{\lambda-1} \cdot \frac{\partial^2 h}{\partial x^2} + \varkappa \cdot \lambda \left(\frac{\partial h}{\partial z}\right)^{\lambda-1} \cdot \frac{\partial^2 h}{\partial z^2} = 0 \qquad (11)$$

Also in this instance, the solutions found will represent flow nets which deviate from those determined on the basis of Darcy's Law.

If Darcy's Law were applicable, a continuity approach for a flow channel would infer a constant lateral component ratio between the individual sections of a flow net:

$$\frac{A_2}{l_2} = \frac{A_1}{l_1} \quad (12)$$

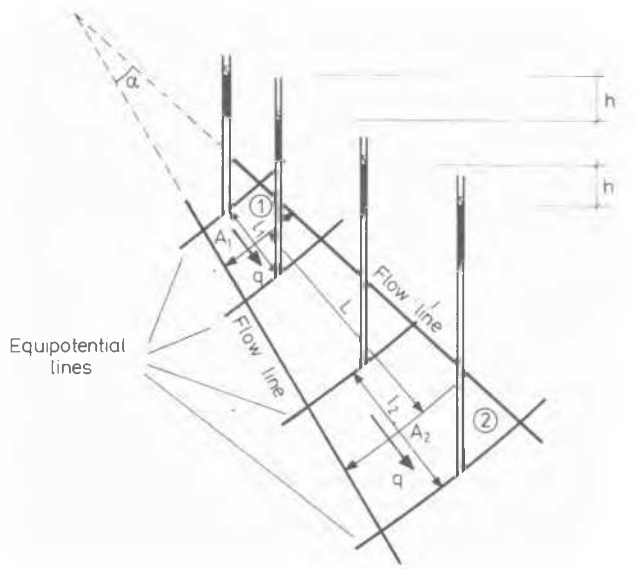

Fig. 10 Simplified flow channel with piezometer pipes for the two-dimensional case

Using equation (1) as a basis for the continuity approach gives:

$$\frac{A_2}{l_2} = \frac{A_1}{l_1} + i_0 \cdot \frac{A_2 - A_1}{h} \quad (13)$$

Here, the ratio of widths and lengths of the various sections of the net remains constant only in the case of an unchanged cross-sectional area ($A_2 = A_1$). The difference of lateral component ratios is equal to the change of cross-sectional area multiplied by factor i_0/h:

$$\frac{A_2}{l_2} - \frac{A_1}{l_1} = (A_2 - A_1) \cdot \frac{i_0}{h} \quad (14)$$

For the widening flow channel with straight-lined boundaries and the aperture angle α shown in Fig. 10, the change of cross-sectional area can be expressed by α in the radian measure and by the center-to-center distance L of the flow net sections as follows:

$$A_2 - A_1 = L \cdot \alpha\ [\text{rad}] \quad (15)$$

From this, it finally results:

$$\frac{A_2}{l_2} = \frac{A_1}{l_1} + \frac{i_0}{h} \cdot L \cdot \alpha[\text{rad}] \quad (16)$$

Analogously, the approach oriented in the direction of a narrowed cross-section gives:

$$\frac{A_2}{l_2} = \frac{A_1}{l_1} - \frac{i_0}{h} \cdot L \cdot \alpha[\text{rad}] \quad (17)$$

The evaluation of equations (16) and (17) resulted in the diagram represented in Fig.11, stating $A_1/l_1 = 1$. Starting from a specific section of the flow net, in this case a square-shaped mesh of the net, the ratios of lateral components are $A_2/l_2 > A_1/l_1$ as seen in the direction of the cross-sectional widening of the flow channel. In the case of narrowing of the cross-section $A_2/l_2 < A_1/l_1$ follow. From this can be inferred that the equipotential lines come closer to each other in the case of increasing cross-section and that the distances between the potential lines become wider in the case of narrowing cross-sections.

When flow channel is widened

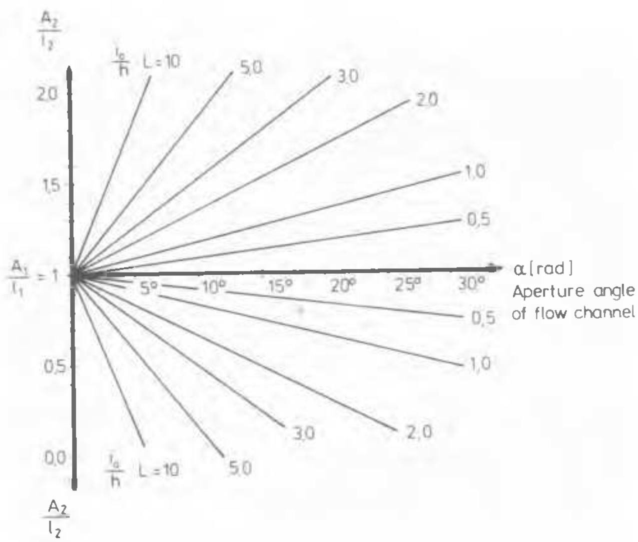

When flow channel is narrowed

Fig. 11 Diagram for the assessment of lateral component ratios of flow net meshwork when $v = k\ (i - i_0)$ is valid

The distance between the potential lines of a mesh gives:

$$l_2 = \frac{h}{\left(\frac{h}{l_1} - i_0\right) \cdot \frac{A_1}{A_2} + i_0} \quad (18)$$

For two adjacent meshes the center-to-center distance is

$$L = \frac{1}{2} \cdot (l_1 + l_2) \quad (19)$$

From this follows for adjacent sections of the net in the case of a narrowing of the flow channel:

$$l_2 = -\frac{1}{2}(l_1 - f^*) \pm \sqrt{[\frac{1}{2}(l_1 - f^*)]^2 - l_1 \cdot f'} \quad (20)$$

and in the case of a widening of the flow channel:

$$l_2 = -\frac{1}{2}(l_1 + f') \pm \sqrt{[\frac{1}{2}(l_1 + f')]^2 + l_1 \cdot f^*} \quad (21)$$

Where:

$$f^* = \frac{h}{i_0} \cdot \left(\frac{2\,A_1}{l_1 \cdot \alpha[rad]} + 1\right) \quad (22)$$

$$f' = \frac{h}{i_0} \cdot \left(\frac{2\,A_1}{l_1 \cdot \alpha[rad]} - 1\right) \quad (23)$$

Using the filtration law (2) for the continuity approach in respect of the flow channel as demonstrated in Fig. 10, the following results:

$$\frac{A_2}{l_2^{\lambda}} = \frac{A_1}{l_1^{\lambda}} \quad (24)$$

$$l_2 = l_1 \cdot \sqrt[\lambda]{\frac{A_2}{A_1}} \quad (25)$$

In this instance also it becomes evident that the potential lines come closer to one another in the case of widening of cross-section and that they come wider apart in the case of narrowing of cross-section.

In comparison to the above, the following is determined for the flow channel shown in Fig. 10 when Darcy's Law and square-shaped meshes of the net are used as a basis:

$$l_{2,D} = l_1 \cdot \frac{1 \pm \frac{1}{2} \cdot \alpha[rad]}{1 \mp \frac{1}{2} \cdot \alpha[rad]} \quad (26)$$

For $|\frac{1}{2} \cdot \alpha[rad]| << 1$ the following applies, by way of approximation:

$$l_{2,D} \approx l_1 \cdot (1 \pm \alpha[rad]) \quad (27)$$

Assuming the constant length of a mesh of the net to be l_1, the calculus for the length of the immediately following mesh on the basis of equation (1) or (2), respectively, and according to Darcy's Law results in a difference of:

$$\Delta l_2 = l_2 - l_{2,D} \quad (28)$$

For n meshes of the flow channel (n - 1) differential amounts of differing magnitudes are determined. In order to determine the difference of the location of the potential line at the extreme end of the n-section, the deviations in the preceding sections are to be added:

$$\Delta l_n = \sum_{i=2}^{n} \Delta l_i \quad (29)$$

CONCLUSIONS

For the purpose of determining the small amounts of seepage water flowing through cohesive soil the statement of modified filtration laws remains without meaning for constructional engineering practice on account of the magnitude of the deviations from Darcy's Law shown above. It is to be noted that even in the case of low hydraulic gradients the flow of water is prevalent and, thus, produces the effect of seepage pressure and that even in the flowless zone at $i > 0$ a corresponding so-called supporting pressure arises.

The application of various filtration laws revealed that different flow nets are obtained and that changes occur in the pattern of water pressure distribution along structures subjected to the flow of water. Comparative calculations performed using the method of finite differences have shown that differences occur especially in the boundary zones of the flow nets where the boundary conditions produce differing effects according to the filtration law stated in each particular case.

Applied to the flow around a building pit wall, an upward flow underneath the building pit bottom has the effect that the potential lines come closer together in the area of the pit wall. From this arise larger hydraulic gradients than those established for a flow net according to Darcy's Law. With regard to hydraulic failure the force of seepage J in the upward direction increases so that in the case of cohesive soil material both the increase of supporting forces through cohesion and through tensile strength, if any, and also the increase of the driving force of seepage through increased gradient are under discussion.

REFERENCES

Davidenkoff, R. (1970). Unterläufigkeit von Stauwerken. Werner-Verlag, Düsseldorf.

Gabener, H.-G. (1983). Untersuchungen über die Anfangsgradienten und Filtergesetze bei bindigen Böden. Bulletins of the Foundation Engineering and Soil Mechanics Section of the University of Essen, Vol. 6, Essen.

Hansbo, S. (1960). Consolidation of Clay, with Special Reference to Influence of Vertical Sand Drains. Swedish Geotechnical Institute, Proceedings No. 18, Stockholm.

Janz, C. (1983). Hydraulischer Grundbruch bei bindigen Böden. Thesis in Foundation Engineering and Soil Mechanics Section of the University of Essen.

Müller-Kirchenbauer, H. (1972). Einflüsse der Filtratbildung auf die Stabilität von Schlitzwänden. Paper presented at Baugrundtagung 1972 in Stuttgart, pp. 843 to 860. Published by Deutsche Gesellschaft für Erd- und Grundbau.

Terzaghi, K./Peck, R.B. (1961). Die Bodenmechanik in der Baupraxis. Springer-Verlag, Berlin/Göttingen/Heidelberg.